PHYSICAL REVIEW B VOLUME 31, NUMBER 10 15 MAY 1985

Ellipsometry and transient reflectivity near the excitonic resonance in CdSe

C. Gourdon and P. Lavallard
Groupe de Physique des Solides de l'Ecole Normale Supérieúre, Université Paris 7, Tour 23, 2 place Jussieu, 75251 Paris Cedex 05, France
(Received 25 July 1984)

We report two experiments. The first is an accurate measurement of the phase of the light reflected by a CdSe crystal in the excitonic region. The second is a direct measurement of the time delay experienced by a reflected wave packet in the same frequency range. We show that it is necessary to take into account the existence of an exciton-free surface layer to satisfactorily fit the experimental results. The very fast variation of phase near the longitudinal exciton frequency, larger than π over 0.3 meV, and the very large delay of 12 ps observed under the same conditions are attributed to multiple reflections inside the exciton-free layer in a frequency range where the layer acts as an antireflecting Fabry-Pérot plate.

I. INTRODUCTION

The propagation of polaritons in semiconductors, i.e., of light coupled to excitons, has been the subject of much theoretical and experimental study.[1,2] As a result of spatial dispersion in the excitonic region, two polariton waves can be created by the incident light and propagate through the crystal at the same frequency, with the same polarization, but with different wave vectors. Maxwell boundary conditions are no more sufficient and one needs[3] an additional boundary condition (ABC) which gives the ratio of the amplitudes of the two polariton waves at the surface of the sample.

Many papers have been published on this problem.[3–12] In the 1970s it was clearly established that the use of the nonlocal nonhomogeneous dielectric susceptibility together with Maxwell's equations is sufficient to derive the right ABC. For some of the authors[4–6] the spatial inhomogeneity is only a consequence of the discontinuity at the surface, and the medium itself is considered homogeneous. Several formulations were proposed but unfortunately experiments did not allow one to make a choice since most of them (reflectivity, transmission, resonant Brillouin scattering, etc.) are quite insensitive to the precise ABC. On the other hand, 20 years ago Hopfield and Thomas[9] suggested that, in the case of Wannier excitons, there should exist at the surface an exciton-free layer (dead layer) whose thickness is roughly equal to the exciton Bohr diameter. They used Pekar's[3] ABC at the interface between the bulk and the dead layer. This model explains well the existence of a spike in the reflectivity curve of some samples.[9,13,14] Recently, increasing attention has been paid to the effects of the surface. Many mechanisms have been considered. They include short-range forces due to the presence of the exciton or the hole at the surface, the image charge potential, and surface electric fields.[10–12] These studies indicate that it is more appropriate to speak of a transition layer where the polarization due to the excitonic contribution gradually vanishes near the surface than to speak of a well-defined dead layer. These models give a better fit with the reflectivity curves than the rough dead-layer model.

Recently, Agrawal *et al.*[15] predicted that, in the cases of CdS and CdSe, transient reflectivity should persist in the excitonic region within about 0.1 ps after the incident light cutoff. Their calculation does not take into account the existence of a dead layer. On the other hand, it is known that the phase derivative with respect to the frequency and the time delay are related by a Fourier transform of the electric field. Nevertheless, Agrawal's prediction does not seem to be in agreement with the previous phase measurement of reflected light achieved in CdS.[16,17]

In this paper we present two kinds of experiments. The first is an accurate measurement of the phase variation with frequency in the excitonic region. The second is a direct measurement of the time delay of the reflected light by an original, though simple, method. All the measurements are done with a cw dye laser. We emphasize that no pulsed source is needed to reveal the transient reflectivity.

In Sec. II we describe the experimental setup for the phase measurement. We then describe the results obtained with a 1.4-μm-thick CdSe sample. As shown in Sec. III, it is necessary to take into account the presence of a dead layer in order to explain our results. We also present a brief survey of a three-layer model (a sample of finite thickness sandwiched between two dead layers). This model gives very good agreement with the experimental data. Section IV concerns the delay measurement.

II. PHASE MEASUREMENT

The light source is a cw dye laser pumped by an argon-ion laser. A Lyot filter in the dye-laser cavity selects first a 0.9-meV spectral width which is narrowed to about 0.03 meV ($\sim$0.01 nm) by means of an etalon in the cavity (Fig. 1). By slightly tilting the plate we can change the incident wavelength. We do measurements every 0.035 meV within about 6 meV. The increment is checked by successively realizing a maximum or a minimum light in-

 ©1985 The American Physical Society

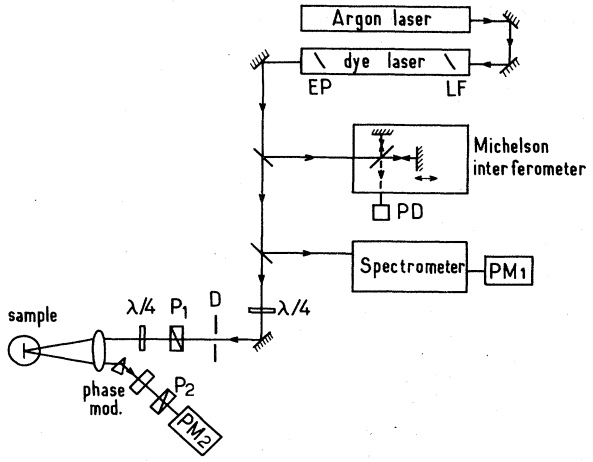

FIG. 1. Experimental setup for phase measurement. LF, Lyot filter; EP, etalon plate; PD, photodiode; PM1 and PM2, photomultipliers; P_1 and P_2, polarizers; D, diaphragm.

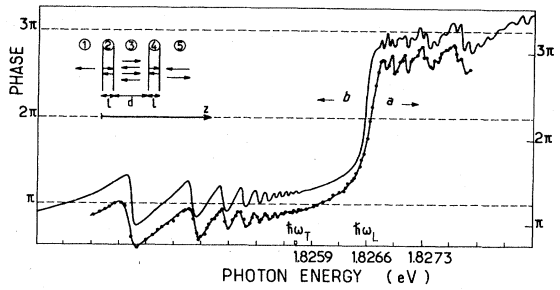

FIG. 2. Phase of reflected light: (a) experimental curve and (b) theoretical curve obtained in a three-layer model. The inset shows the layers: media 1 and 5 correspond to vacuum, media 2 and 4 are the exciton-free layers, and medium 3 is the bulk sample.

tensity at the output of a Michelson interferometer adjusted to give constructive interferences every 0.070 meV ($\sim$0.025 nm).

The lowest-energy excitonic transition is allowed only with a light polarization $\mathbf{E}\perp\hat{\mathbf{c}}$. The $\mathbf{E}\|\hat{\mathbf{c}}$ component of the light is affected by a phase variation almost independent of the frequency in the excitonic region and roughly equal to π. Likewise, the amplitude remains almost constant. We can take the phase of this component, $\phi_{\|}$, as a reference for the variation of the phase $\phi_{\perp}$ of the $\mathbf{E}\perp\hat{\mathbf{c}}$ component. For each frequency ν we compensate the phase variation $\phi_{\perp}(\nu)-\phi_{\|}$ by means of a polarizer P_1 followed by a quarter-wave plate whose axes are at 45° to the c axis. Here, P_1 is rotated off an angle ψ with respect to the quarter-wave-plate axes. The ellipticity cancels out when $\psi=[\phi_{\|}-\phi_{\perp}(\nu)]/2$.

As the amplitude reflection coefficient $\rho_{\perp}$ varies with ν, the direction of the linearly polarized reflected light (after cancellation) also varies with ν. Thus the problem is to establish that the reflected light is linearly polarized whatever its direction. This is achieved by means of an elasto-optic modulator followed by an analyzer. A detailed description is given in Ref. 16. At each frequency the angular position of the polarizer P_1 is adjusted to obtain a zero signal on the output of a lock-in amplifier whose reference signal is provided by the elasto-optic modulator. The laser beam, initially linearly polarized, passes through a quarter-wave plate positioned before the polarizer P_1. This prevents the intensity from varying too much as one rotates this polarizer. The light is focused on the sample by a 10-cm-focal-length lens. The reflected beam is made parallel to the incident one by having it pass through the same lens. The spot on the sample is about 100 μm in diameter. The adjustment of its position over the best part of the sample surface is checked by looking through a microscope lens placed behind it. The sample is freely mounted in a paper bag immersed in pumped liquid helium at about 2 K. In order to avoid any cause of unwanted ellipticity, we used no mirrors between the first polarizer P_1 and the photomultiplier. The reflected light was deviated by a prism. We also replaced the screwed windows of the cryostat, which caused some birefringence, by a plane-parallel-faced cell. The results obtained with a 1.4-μm-thick sample are shown in Fig. 2. The change of phase throughout the transition is equal to 2π. Close to the longitudinal frequency ν_L the curve exhibits a very fast variation of the order of π over 0.3 meV. As the sample is very thin, we can observe the Fabry-Pérot interferences together with the additional wave interferences (mainly above ν_L). This is in good agreement with the reflection and transmission spectra obtained simultaneously on the same sample. Some other samples give the same kind of phase curve. From now on we shall refer to them as "S"-type phase curves, yet a thicker one (probably of poorer quality) yielded a different curve (Fig. 3). On the low-energy side of the transition the phase is slightly greater than π; it increases with the frequency, then decreases abruptly near the longitudinal frequency ν_L, and arrives at a final value slightly smaller than π at higher frequency. This kind of curve will be referred to as an "N"-type phase curve.

III. THEORETICAL MODEL

In order to explain our results we first consider a model with a simple vacuum-sample interface. The sample is as-

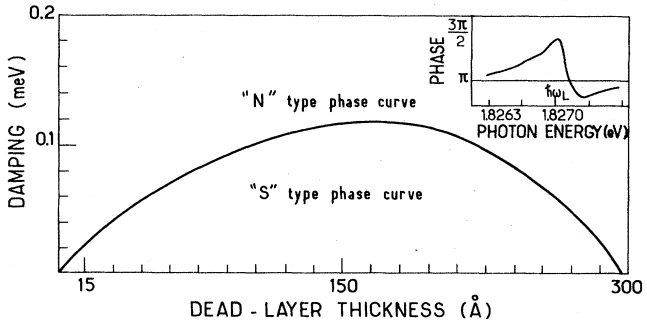

FIG. 3. Ranges of the parameters Γ and l corresponding to different types of solutions for $\phi(\nu)$. Inset: N-type curve of a thick sample ($\simeq$30 μm).

sumed to be a semi-infinite medium in the z direction. Let us consider four ABC's as given in the literature: We have

$$\text{(i)}\quad P\,|_{\Sigma}=0 \tag{1}$$

(Pekar's ABC[3]), or

$$(n_1^2-\epsilon_\infty)E_1+(n_2^2-\epsilon_\infty)E_2=0$$

at the surface Σ. P is the excitonic contribution to the polarization. E_1 and E_2 and n_1 and n_2 are the electric fields and the complex refractive indices corresponding to the two polariton branches, respectively. We then have

$$\text{(ii)}\quad \left.\frac{\partial P}{\partial z}+ik_+P\right|_{\Sigma}=0 \quad\text{or}\quad \frac{E_1}{n_1-n_+}+\frac{E_2}{n_2-n_+}=0\,, \tag{2}$$

with

$$k_+^2=\left[\frac{n_+\omega}{c}\right]^2=\frac{m^*}{\hbar\omega_T}(\omega^2-\omega_T^2+i\Gamma\omega)\,,$$

where m^* is the effective exciton mass, ω_T is the transverse exciton angular frequency, and Γ is the phenomenological damping. This ABC is given by several authors.[4–6] Next, we have

$$\text{(iii)}\quad \left.\frac{\partial P}{\partial z}\right|_{\Sigma}=0 \quad\text{or}\quad n_1(n_1^2-\epsilon_\infty)E_1+n_2(n_2^2-\epsilon_\infty)E_2=0\,, \tag{3}$$

given by Ting *et al.*[7] in case of Wannier excitons. Finally, we have

$$\text{(iv)}\quad \left.\frac{\partial P}{\partial z}+\frac{\omega}{\gamma c}P\right|_{\Sigma}=0$$

or

$$(1+\gamma n_1)(n_1^2\epsilon_\infty)E_1+(1+\gamma n_2)(n_2^2-\epsilon_\infty)E_2=0\,, \tag{4}$$

used by Kiselev[8] with $\gamma=10^{-2}$.

The curves which correspond to these ABC's are shown in Fig. 4. They are all very similar. None of them can reproduce the S-type curve we obtained with the best samples.

On the other hand, the dead-layer model gives good agreement with the experimental data. The exciton-free layer has a refractive index $n_\infty=(\epsilon_\infty)^{1/2}$. We use Pekar's ABC at the interface between the dead layer and the semi-infinite medium. This is equivalent to taking the effective complex refractive index n_3, given by

$$n_3=\frac{n_1n_2+\epsilon_\infty}{n_1+n_2}\,.$$

The phase ϕ of the reflected wave is calculated by considering multiple reflections inside the dead layer.

Depending on the values of the dead-layer thickness l and the damping coefficient Γ, we can obtain either an S- or an N-type phase curve (Fig. 5). The change from one type of curve to the other occurs with some critical values of l and Γ. The corresponding curve is shown in Fig. 3. In the upper part of the plane the curves are of N type, whereas in the lower part they are of S type. For the critical values of the parameters Γ and l, the derivative $\partial\phi/\partial\nu$ becomes infinite at a frequency ν_c very close to ν_L.

Let $r_{12}=\rho_{12}\exp(i\phi_{12})=-|\rho_{12}|$ be the reflection coefficient at the vacuum–dead-layer interface, and let $r_{23}=\rho_{23}\exp(i\phi_{23})$ be the reflection coefficient at the dead-layer–medium interface, with

$$r_{23}=\frac{n_\infty-n_3}{n_\infty+n_3}\,.$$

Two conditions are fulfilled at the critical frequency ν_c, namely

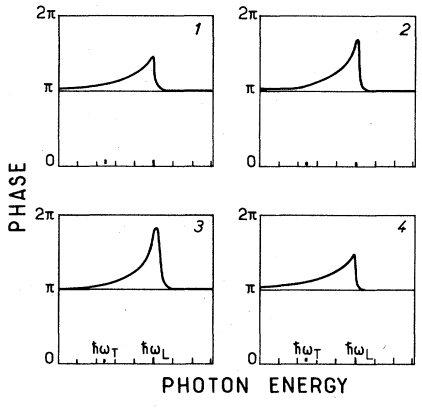

FIG. 4. Phase of light reflected from a semi-infinite sample. The four different cases correspond to different ABC's (see text). No dead layer is taken into account.

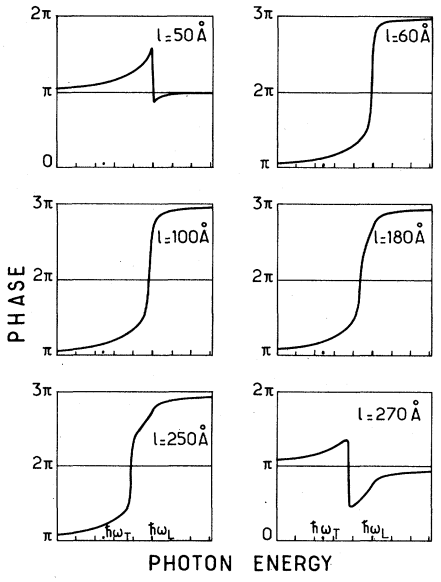

FIG. 5. Phase of light reflected from a semi-infinite sample with a dead-layer of thickness l. The parameters ϵ_∞, $\hbar(\omega_L-\omega_T)$, and Γ are given in the text.

$$\rho_{23}(\nu_c)=|r_{12}| \quad \text{and} \quad \phi_{23}(\nu_c)+2\beta=2\pi ,$$

where $\beta=2\pi n_\infty l/c$ is the phase shift due to the dead layer. Under these conditions the dead layer acts as a very thin Fabry-Pérot plate at the reflection minimum, and destructive interferences occur between the first reflected ray and all the others. As a result, the reflectivity curve has a minimum equal to zero at frequency ν_c.[18] In our case the two conditions are not fulfilled at the same frequency, but rather for frequencies ν_{c1} and ν_{c2} very close to each other and to ν_L.

The first reflected ray and all the others can be considered as two vectors in the complex plane. The very small resulting sum represents the amplitude and phase of reflected light. It rotates quickly with frequency when ν is close to either ν_{c1} or ν_{c2}. This explains the very fast change of phase close to the longitudinal exciton frequency. Of course, our simple model can only give the general shape of the phase curve and not the interference pattern since it does not take into account the sample thickness. A three-layer model requires a more sophisticated theoretical treatment since the total electromagnetic field inside each layer is the sum of two counterpropagating fields. The impedance method[19] is very convenient in solving such a problem.

The inset of Fig. 2 shows the three layers. Media 1 and 5 correspond to vacuum, layers 2 and 4 are the dead layers of thickness l and refractive index $n_\infty=(\epsilon_\infty)^{1/2}$, and layer 3 is the bulk medium of thickness d.

We start from the last interface, where the input impedance (the ratio of the electric field and the magnetic field) is simply equal to the impedance of the medium, $Z=1/N$, where N is the complex refractive index of the layer. We calculate the electric field and the magnetic field at the next interface by taking into account the phase shift and the attenuation of the waves in the layer. In the central layer the problem is complex since two waves can propagate. The calculation of the input impedance is done by simultaneously considering Pekar's condition and Maxwell's boundary conditions. We finally obtain the complex reflection coefficient $r=|r|e^{i\phi}$ and thus the phase ϕ of the reflected wave. The calculations are given in Ref. 20.

To make a comparison with the experiments, we used parameters which are close to those given elsewhere,[8] that is, $\epsilon_\infty=8.1$, $\hbar\omega_L=1.8266$ eV, and $\hbar(\omega_L-\omega_T)=9\times10^{-4}$ eV. From the best fit of the experimental and theoretical curves of reflection and transmission, we obtained a sample thickness of (1.4 ± 0.02) μm and a damping factor of $(5\pm1)\times10^{-5}$ eV. In fact, there is a slight discrepancy between the best values of Γ for the reflectivity and the phase curves, especially above ω_L. Thus we think that the use of a frequency-dependent Γ, as proposed in Ref. 21, could improve the fit between the theoretical and experimental curves. Figure 2(b) shows the theoretical curve calculated with a dead-layer thickness $l=100$ Å. The dead-layer—thickness determination is not very precise because the phase curve does not change very much with the parameters Γ and l when their values are not close to the critical ones. The order of magnitude of the thickness is in good agreement with Hopfield's evaluation of a intrinsic dead layer $l\sim2r_B$, r_B being the exciton Bohr radius. Nevertheless, we cannot exclude an extrinsic contribution.

IV. TIME BEHAVIOR OF THE REFLECTED WAVE

In addition to the phase measurement, we studied the time behavior of the reflected wave by an interferometric method. We perform, after reflection on the sample surface, a cross correlation of the two components of the incident electric field, one parallel to the c axis and the other perpendicular to it. The discrimination is achieved by placing two polarizers at 90° in the two arms of a Michelson interferometer (Fig. 6). A half-wave plate is used to precisely align these two polarization directions with the c axis of the sample and the direction perpendicular to it. The vibration with $\mathbf{E}\perp\hat{\mathbf{c}}$ travels through the arm ending in the mobile mirror. After reflection on the sample, the two vibrations are recombined on an analyzer which is adjusted to give them equal amplitudes. The oscillation term in the resulting intensity is

$$I(\tau)=\int E_{\parallel}^{R}(t)E_{\perp}^{R}(t-\tau)dt ,$$

where τ is the delay due to the different path lengths in the two interferometer arms. $E_{\parallel}^{R}$ and $E_{\perp}^{R}$ are the amplitudes of the reflected light polarized parallel and perpendicular to the c axis, respectively. The envelope of these interferences is recorded relative to the position of the mobile mirror. The link with the frequency domain is obvious since one can write

$$I(\tau)=\int_0^\infty a_{\parallel}^{R}(\nu)a_{\perp}^{R}(\nu)\cos[2\pi\nu\tau+\phi(\nu)]d\nu ,$$

where $a_{\parallel}^{R}(\nu)$ and $a_{\perp}^{R}(\nu)$ are the frequency spectra of $E_{\parallel}^{R}$ and $E_{\perp}^{R}$, and $\phi(\nu)=\phi_\perp(\nu)-\phi_\parallel$ is the phase difference between the two electric fields. When the phase variation of the electric field can be described simply by a delay, the shift of the peak of the interference-envelope curve then gives a direct measurement of it (we must compensate for the delay experienced by the $\mathbf{E}\perp\hat{\mathbf{c}}$ vibration at the reflection on the sample by providing for a shorter propagation time in one interferometer arm). Let us call $r_\perp(\nu)=\rho_\perp(\nu)\exp[i\phi_\perp(\nu)]$ the complex reflection coefficient for the amplitude of the $\mathbf{E}\perp\hat{\mathbf{c}}$ vibration. For the sake of simplicity, let us assume that $\rho_\perp(\nu)$ is almost independent of ν and that $\phi_\perp(\nu)$ varies linearly with ν about the mean frequency ν_0 of the laser light, at least in a narrow frequency range. It is then easy to see that the derivative of the phase with ν around ν_0 is equivalent to a time delay, i.e.,

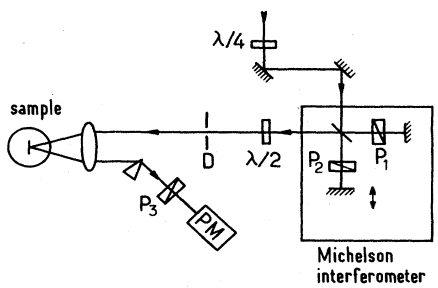

FIG. 6. Experimental setup for time-delay measurement. P_1, P_2, and P_3 are polarizers. P_1 and P_2 are orthogonal. D is a diaphragm.

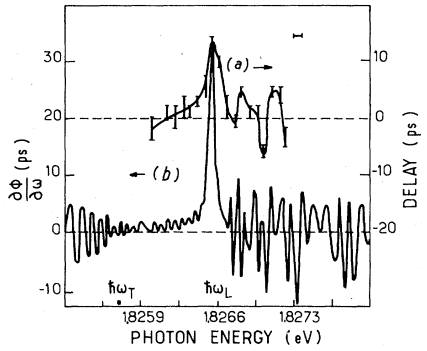

FIG. 7. Time delay of reflected light: (a) experimental curve, and (b) theoretical curve obtained with a three-layer model.

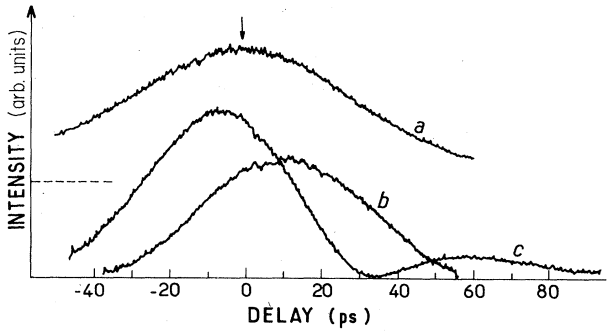

FIG. 8. Cross correlation of the $\mathbf{E}\|\hat{\mathbf{c}}$ and $\mathbf{E}\perp\hat{\mathbf{c}}$ components of the wave packet: (a) before sample, (b) after sample with $\hbar\omega_b = 1.8265$ eV, and (c) after sample with $\hbar\omega_c = 1.8270$ eV.

lay, i.e.,

$$\tau = \frac{1}{2\pi}\frac{\partial\phi_\perp}{\partial\nu}\bigg|_{\nu_0}.$$

The spectral width of the laser is taken to be 0.06 meV. The corresponding coherence time (70 ps) allows us to measure a delay of a few picoseconds. But the delay measurement is then less accurate than the phase measurement. Experimental and theoretical curves are shown in Fig. 7. We observe a maximum experimental delay of 12 ps at the frequency corresponding to the maximum slope of the phase curve. The very long delay can be explained as previously by the multiple reflections in the dead layer. The delay introduced through the dependence of ϕ_{23} on ν, already greater than that for an ordinary medium, is enhanced at each reflection.

Above ν_L, in a narrow frequency range, the envelope curve of the interferences exhibits two maxima (Fig. 8). Since the phase curve in this frequency region shows a fine structure due to the interferences with the additional wave, it can no longer be assumed that the phase variation is linear with frequency. From the known thickness of the sample (1.4 μm) one can calculate that the time delay corresponding to the second peak (60 ps) is roughly equal to the time of flight of a wave packet produced with the lower polariton branch.[22] We interpret, then, the second maximum of the envelope curve as being due to a round trip in the sample, one way as a lower polariton wave (very small delay) and the other as an upper polariton wave (60-ps time delay). On the other hand, the first peak appears slightly in *advance* with respect to the zero delay (Fig. 8). This is not so paradoxical since we consider only the peak of the signal. Theoretical investigations of pulse propagation in dispersive and absorbing media have been carried out by Garrett and McCumber[23] and by Crisp.[24] Crisp shows that, because of the finite response time of the medium, polarization depends both on the amplitude E of the envelope of the incident pulse and its derivative, $\partial E/\partial t$. The field radiated by the excited dipoles is then different when they are excited by the front edge or the trailing edge of the pulse. Thus the maximum of the reflected pulse may be either advanced or delayed with respect to the maximum of the incident one. This effect is important when the absorption length is of the order of the dimension of the pulse or the wave packet in the medium.

V. CONCLUSION

Through a very accurate phase measurement of the reflected light in the excitonic region of a CdSe sample, we showed that it is necessary to take into account the existence of a dead layer in order to achieve a satisfactory fit of the experimental results. We attribute the very fast variation of phase about the longitudinal exciton frequency to the Fabry-Pérot effect of this dead layer. We are aware that this model remains a rough approximation and that a transition layer as described in the Introduction is certainly a better description of the surface region. However, there is usually little discrepancy between the two descriptions for excitons of small Bohr radius.[10] Since we obtain good agreement with the dead-layer model, we think that, at least in CdSe, this model is an adequate one.

Furthermore, the transient reflectivity was studied by a very simple interferometric method. The results are in agreement with the phase measurements. We were able to measure a delay as large as 12 ps and demonstrate the existence of two wave packets propagating at different velocities.

We stress that in a reflectivity or transmission experiment the output beam maintains a phase relation with the incident beam. Transient measurements can thus be performed with a continuous wave.

[1]J. L. Birman, in *Excitons,* edited by E. I. Rashba and M. D. Sturge (North-Holland, Amsterdam, 1982), Chap. 1.
[2]E. L. Ivchenko, in *Excitons,* Ref. 1, chap. 4.
[3]S. I. Pekar Zh. Eksp. Teor. Fiz. **33**, 1022 (1957) [Sov. Phys.—JETP **6**, 785 (1958)].
[4]J. L. Birman and J. J. Sein, Phys. Rev. B **6**, 2482 (1972).
[5]A. A. Maradudin and D. L. Mills, Phys. Rev. B **7**, 2787 (1973).
[6]G. S. Agarwal, D. N. Pattanayak, and E. Wolf, Phys. Rev. B

10, 1447 (1974).

[7]C. S. Ting, M. J. Frankel, and J. L. Birman, Solid State Commun. **17**, 1285 (1975).

[8]V. A. Kiselev, B. S. Razbirin, and I. N. Uraltsev, Phys. Status Solidi B **72**, 161 (1975).

[9]J. J. Hopfield and D. G. Thomas, Phys. Rev. **132**, 563 (1963).

[10]I. Balslev, Phys. Status Solidi B **88**, 155 (1978); Phys. Rev. B **23**, 3977 (1981).

[11]J. Lagois, Phys. Rev. B **23**, 5511 (1981).

[12]A. D'Andrea and R. Del Sole, Phys. Rev. B **25**, 3714 (1982).

[13]F. Evangelisiti, A. Frova, and F. Patella, Phys. Rev. B **10**, 4253 (1974).

[14]G. V. Benemanskaya, B. V. Novikov, and A. E. Cherednichenko, Fiz. Tverd. Tela (Leningrad) **19**, 1389 (1977) [Sov. Phys.—Solid State **19**, 806 (1977)].

[15]P. G. Agrawal, J. L. Birman, D. N. Pattanayak, and A. Puri, Phys. Rev. B **25**, 2715 (1982).

[16]A. V. Komarov, S. M. Ryabchenko, and M. I. Strashnikova, Zh. Eksp. Teor. Fiz. **74**, 257 (1978) [Sov. Phys.—JETP **47**, 128 (1978)].

[17]A. B. Pevtsov, S. A. Permogorov, Sh. R. Saifullaev, and A. V. Sel'kin, Fiz. Tverd. Tela (Leningrad) 22, 2400 (1980) [Sov. Phys.—Solid State **22**, 1396 (1980)].

[18]Let us point out that the vanishing of the reflectivity, together with the change of the phase curve shape, can be described as the normal incidence Brewster effect (A. B. Pevtsov and A. V. Sel'kin, Zh. Eksp. Teor. Fiz. **83**, 516 (1982) [Sov. Phys.—JETP **56**, 282 (1982)]).

[19]L. M. Brekhovskikh, in *Waves in Layered Media*, edited by R. T. Beyer (Academic, New York, 1960).

[20]C. Gourdon, thèse de troisième cycle, Université Paris VI, 1984.

[21]T. Shigenari, X. Z. Lu, and H. Z. Cummins, Phys. Rev. B **30**, 1962 (1984).

[22]P. H. Duong, T. Itoh, and P. Lavallard, Solid State. Commun. **43**, 879 (1982).

[23]C. G. B. Garrett and D. E. McCumber, Phys. Rev. A **1**, 305 (1970).

[24]M. D. Crisp, Phys. Rev. A **1**, 1604 (1970).